

Accepted Manuscript

Clomiphene citrate induces nuclear translocation of the TFEB transcription factor and triggers apoptosis by enhancing lysosomal membrane permeabilization

Wei Li, Jieru Lin, Zhichen Shi, Jiren Wen, Yuyin Li, Zhenxing Liu, Aipo Diao

PII: S0006-2952(18)30494-5
DOI: <https://doi.org/10.1016/j.bcp.2018.11.016>
Reference: BCP 13359

To appear in: *Biochemical Pharmacology*

Received Date: 28 September 2018
Accepted Date: 20 November 2018

Please cite this article as: W. Li, J. Lin, Z. Shi, J. Wen, Y. Li, Z. Liu, A. Diao, Clomiphene citrate induces nuclear translocation of the TFEB transcription factor and triggers apoptosis by enhancing lysosomal membrane permeabilization, *Biochemical Pharmacology* (2018), doi: <https://doi.org/10.1016/j.bcp.2018.11.016>

This is a PDF file of an unedited manuscript that has been accepted for publication. As a service to our customers we are providing this early version of the manuscript. The manuscript will undergo copyediting, typesetting, and review of the resulting proof before it is published in its final form. Please note that during the production process errors may be discovered which could affect the content, and all legal disclaimers that apply to the journal pertain.



Clomiphene citrate induces nuclear translocation of the TFEB transcription factor and triggers apoptosis by enhancing lysosomal membrane permeabilization

Wei Li^{a,b}, Jieru Lin^a, Zhichen Shi^a, Jiren Wen^a, Yuyin Li^a, Zhenxing Liu^{a,*}, Aipo Diao^{a,*}

^a School of Biotechnology, Tianjin University of Science and Technology, Key Lab of Industrial Fermentation Microbiology of the Ministry of Education, Tianjin 300457, China

^b School of Basic Medical, Inner Mongolia Medical University, Hohhot 010110, Inner Mongolia, China

* **Corresponding author at:** School of Biotechnology, Tianjin University of Science and Technology, Tianjin 300457, China.

Email address: diaoaiipo@tust.edu.cn (Aipo Diao); liuzx@tust.edu.cn (Zhengxing Liu)

ABSTRACT

The autophagy-lysosome pathway plays a central role in cellular homeostasis by regulating the cellular degradative machinery. The transcription factor EB (TFEB) regulates the biogenesis and function of both lysosomes and autophagosomes, and enhancement of TFEB function has emerged as an attractive therapeutic strategy for lysosome-related disorders. However, little is known about the role of TFEB activation in regulating the cellular fate. Here, we describe that clomiphene citrate (CC), a selective estrogen receptor modulator, promotes nuclear translocation of TFEB and increases lysosomal biogenesis in HeLa and MDA-MB-231 cells. Treatment with CC inhibits cell viability and causes apoptosis by increasing the release of proteases cathepsin B (CatB) and cathepsin D (CatD) from lysosomes into the cytosol. In contrast, knockdown of TFEB rescues the cells from CC-induced cell death. Furthermore, CC-induced TFEB activation also enhances the autophagy flux in HeLa cells. Knockdown of autophagy-related gene 7 (ATG7) significantly decreases the CC-induced CatB and CatD release and cell death, suggesting that autophagy contributes to the lysosomal membrane permeabilization (LMP) caused by CC. Altogether, these findings have broad implications for our understanding of TFEB function and provide new insights into CC pharmacological therapy.

Key words: TFEB, Clomiphene citrate, Lysosome, Apoptosis, Autophagy

1. Introduction

Lysosomes are ubiquitous organelles containing many acid hydrolase and function as the cellular digestive organ. Autophagy is a well-conserved mechanism that is activated in response to nutrient deprivation and is a highly regulated process for degradation of macromolecules via the lysosome. The autophagy-lysosome degradative pathway plays a central role in cellular homeostasis through which protein aggregates, damaged organelles and intracellular pathogens are sequestered by autophagosomes and degraded by lysosomes, resulting in nutrient recycling and energy regeneration[1]. Impairment of this machinery has been associated with multiple diseases such as lysosomal storage disorders (LSDs), neurodegenerative diseases, metabolic symptoms and ageing[2-4]. Knockout of autophagy-related gene 7 (ATG7) in mice, an essential autophagy gene, led to glucose intolerance and susceptibility to diabetes due to structural and functional defects of pancreatic β -cells[5, 6]. In metabolic syndromes such as obesity and fatty liver, defective autophagy-lysosome machinery results in aggregation of macromolecules (lipids, proteins, and glycogen) and impaired organelles, which damages metabolic activity at the tissue level, promotes endoplasmic reticulum (ER) stress, and causes insulin resistance[3, 7, 8]. Within age-related disorders, a deficient autophagy-lysosome pathway impairs the clearance of defective organelles, resulting in pathological accumulation of proapoptotic factors and reactive oxygen species (ROS)[4, 9]. In contrast, overexpression of autophagy-related gene 5 (ATG5), another essential autophagy gene, activates autophagy and extends the lifespan of aged mice[10]. Therefore, pharmacological interventions that enhance autophagy-lysosome clearance have

emerged as an attractive therapeutic strategy to ameliorate metabolic and age-related disorders.

Transcription factor EB (TFEB), a master regulator for lysosomal biogenesis, modulates lysosomal biogenesis and autophagy by positively regulating genes belonging to the Coordinated Lysosomal Expression and Regulation (CLEAR) network[[11-13](#)]. TFEB is a member of the basic helix-loop-helix leucine-zipper family that recognizes a 10-base pair motif (5'-GTCACGTGAC-3') enriched in the promoter regions of numerous lysosomal genes[[11](#)]. Under conditions of amino acid satiety, TFEB is recruited to lysosomal membranes by the Rag GTPases-Ragulator complex, allowing for its phosphorylation at serine 211 by mammalian target of rapamycin complex 1 (mTORC1)[[14-16](#)]. Phosphorylated TFEB is sequestered by chaperones of the 14-3-3 family, which actively prevent its translocation to the nucleus[[15, 16](#)]. Under starvation conditions, inactivation of mTORC1 allows nuclear translocation of TFEB to mediate cellular adaptation to stress by promoting lysosomal biogenesis, autophagy induction, as well as expression of critical mitochondrial and metabolic regulators[[11, 16-19](#)]. Moreover, activation of TFEB transactivates genes necessary for autophagosome formation, autophagosome-lysosome fusion, and cargo degradation[[13, 17](#)]. TFEB overexpression induces an increase in the number of autophagosomes and autophagic flux, and leads to the clearance of storage cargo in multiple LSDs by promoting lysosomal secretion[[13, 20](#)]. Therefore, TFEB agonists are of interest for potential therapeutic intervention for some metabolic disorders or ageing. Recently, several TFEB activators have been identified for the treatment of metabolic syndrome and neurodegenerative disease in mice[[21-23](#)]. However, relatively little is known about the

negative role of TFEB activation in the control of cellular fate such as growth inhibition and apoptosis.

The clomiphene citrate (CC), a selective estrogen receptor modulator (SERM), is used for the induction of ovulation in anovulatory women[24]. Chemically, CC is a nonsteroidal triphenylethylene derivative that exhibits both estrogen agonist and antagonist properties[25]. CC induces cytotoxicity such as generation of ROS and apoptosis in cancer cells[26], perturbations during meiotic maturation of oocytes[27], and apoptosis in granulosa cells and oocytes[28]. In addition to its modulation of estrogen receptors, CC also binds to the microsomal antiestrogen binding site (AEBS) with high affinity[29]. It has been reported that CC and other AEBS ligands induce breast cancer cell differentiation, apoptosis and autophagy through the modulation of cholesterol metabolism[30]. However, it remains unclear whether CC or AEBS ligands induced cellular effects are associated with TFEB.

In this study, we have identified CC as a small-molecule TFEB agonist, which promotes nuclear translocation of TFEB, resulting in an increased number of lysosomes and autophagic flux. Further, we found that CC-mediated activation of TFEB reduced cell viability and induced apoptosis by enhancing lysosomal membrane permeabilization (LMP). These findings provide insights into our understanding of TFEB function and CC pharmacological therapy.

2. Materials and methods

2.1. Cell culture and reagents

All cell lines were obtained from the American Type Culture Collection (ATCC). The cells were routinely cultured in DMEM (Gibco, Eggenstein, Germany) containing 10% fetal bovine serum (Gibco), 100 U/mL penicillin and 0.1 mg/mL streptomycin in a humidified cell incubator with an atmosphere of 5% CO₂ at 37 °C. All chemicals were purchased from Sigma Aldrich (St. Louis, MO, USA) unless otherwise stated. Antibodies against TFEB (sc-48784), cathepsin D (CatD) (sc-6486), β -actin (sc-47778) and Lamin A/C (sc-7293) were obtained from Santa Cruz Biotechnology (Santa Cruz, CA, USA). Antibodies against cleaved caspase-9 (#9501), cleaved caspase-3 (#9664), phospho-p70S6K (#9202), ATG7 (#8558) and p62 (#5114) were purchased from Cell Signaling Technology (Danvers, MA, USA). Antibodies against cathepsin B (CatB) (ab190077), LAMP-2 (ab25631) were purchased from Abcam (Cambridge, UK). Anti-LC3B (L7543) antibody was from Sigma. Antibody against GAPDH (B1034) was purchased from Biodragon (Beijing, China). Antibody against ER α (AE905) was purchased from Beyotime (Shanghai, China). Antibody against GFP (KM8009) and the horseradish peroxidase (HRP)-conjugated goat anti-rabbit (LK2001) or anti-mouse (LK2003) secondary antibodies were purchased from Sungene Biotech (Tianjin, China). Clomiphene citrate (purity 99.46%) and Torin1 (purity 99.01%) were obtained from Selleckchem (Houston, TX, USA). Tamoxifen (purity \geq 98%) was obtained from TargetMol (Boston, MA, USA). FITC Annexin V apoptosis Detection Kit and Propidium Iodide (PI) were purchased from BD Pharmingen (Franklin Lakes, NJ, USA).

2.2. Plasmid construction and stable cell line

The full length of human TFEB (GenBank accession no. NM_001167827.2) was amplified by PCR using forward (5'-CGGAATTCTGATGGCGTCACGCATAGGGTTGC-3') and reverse (5'-CGGGATCCCGCAGCACATCGCCCTCCTCCATG-3') primers, and the cDNAs obtained from HeLa cells as the template. The PCR fragments of TFEB digested with EcoRI and BamHI (New England Biolabs, Ipswich, MA, USA) were cloned into pLVX-AcGFP-N1 plasmid (Clontech, Palo Alto, CA, USA) for generation of the TFEB-GFP transfection vector. A plasmid that encoded human microtubule-associated protein 1 light chain 3 (LC3; GenBank accession no. NM_022818.4) tagged with GFP (GFP-LC3) was generated in pLVX-AcGFP-C1 plasmid at the XhoI and BamHI sites using the same cDNA library and specific forward (5'-TTCTCGAGCTATGCCGTCGGAGAAGA-3') and reverse (5'-AAGGATCCTTACTGACAATTTTCATCC-3') primers for PCR amplification. All constructs were verified by DNA sequencing. The Lentivirus particles were generated by transfecting HEK-293T cells with pMD2.G and psPAX2 packaging plasmids and the corresponding backbone plasmid using Lipofectamine 2000 (Invitrogen, Carlsbad, CA, USA) according to the manufacturer's instructions. Viruses were collected 48 h post-transfection, and used for infection overnight in the presence of 8 µg/mL polybrene. HeLa cells stably expressing TFEB-GFP or GFP-LC3 was obtained by infection with pLVX-AcGFP-TFEB or pLVX-AcGFP-LC3 lentiviruses and selected in 1 µg/ml puromycin for at least two weeks.

2.3. Cytoplasmic protein extraction, nuclear and cytoplasmic fractionation

Cells were harvested, washed with Dulbecco's Phosphate Buffered Saline (DPBS) and resuspended in 1 mL cytosol extraction buffer (250 mM sucrose, 20 mM Hepes, 10 mM KCl,

1.5 mM MgCl₂, 1 mM EDTA, 1 mM EGTA, 25 g/ml digitonin, 1 mM PMSF, pH 7.5) on ice for 30 min. After spinning at 14000 rpm for 10 min, the supernatant was removed to a new tube and 100% Trichloroacetic acid (TCA) was added (10% final concentration) dropwise, and rotated slowly at 4 °C overnight. After spinning for 15 min at 14000 rpm, the supernatant was discarded and 0.8 mL of 100% chilled acetone was added to the pellet. The pellet was dried and resuspended in SDS-PAGE sample buffer. Ammonia vapour was added to neutralize the pH and the sample was boiled prior to gel loading. Subcellular fractionation of cells was performed using the NE-PER Nuclear and Cytoplasmic Extraction Kit (Thermo Scientific, Waltham, MA, USA) according to the manufacturer's instructions. Briefly, cells were homogenized in cytoplasmic extraction reagent I with subsequent addition of cytoplasmic extraction reagent II. The supernatants after the centrifugation step represented the cytoplasmic fractions. The insoluble pellets were suspended in nuclear extraction reagent, and nuclear proteins were extracted by centrifugation.

2.4. Western blot

Cell lysates were prepared by extracting proteins with RIPA buffer (Sigma) containing protease cocktail inhibitor (Roche, Basel, Switzerland). Equal amounts of protein samples were subjected to SDS-PAGE and transferred onto a nitrocellulose membrane (Millipore, Billerica, MA, USA). After blocking with 5% non-fat milk in Tris-buffered saline containing 0.1% Tween-20 (TBST), the membrane was incubated with primary antibodies diluted in blocking solution at 4°C overnight. After washing with TBST, the membrane was incubated for an additional 2 h with the appropriate secondary antibodies conjugated to HRP. The

immunoblot bands were visualized using a chemiluminescence detection system (GE Healthcare, Little Chalfont, Buckinghamshire, UK). The density of the bands were analyzed using ImageJ software (Wayne Rasband, NIH, Bethesda, MD, USA).

2.5. Cell viability assay

Cells were seeded in 96-well plates at a density of 5×10^3 cells per well. After CC treatment, cell viability was assessed using 3-(4,5-dimethylthiazol-2-yl)-2,5-diphenyl tetrazolium bromide (MTT) (Solarbio, Beijing, China) dye absorbance and expressed as the percentage of non-treated cells. Briefly, after exposure of cells to CC, MTT solution (20 μ L, 0.5 mg/mL in PBS) was added and incubated at 37 °C for 4 h. Then, DMSO (200 μ L/well) was added to dissolve the formazan dyes and the absorbance was measured at 490 nm using a microplate reader (Bio-Rad, Hercules, CA, USA).

2.6. Apoptosis analysis

Cells were plated on 60-mm dishes for 12 h, and then treated with CC. Cells were harvested, washed twice with ice-cold PBS, and evaluated for apoptosis by double staining with FITC conjugated Annexin V and PI in binding buffer for 30 min using a FACSCalibur flow cytometer (BD Biosciences, CA, USA). The percentage of apoptosis was calculated and analyzed by early apoptosis and late apoptosis (Q2 phase + Q3 phase). For TdT-mediated dUTP nick-end labeling (TUNEL) staining, cells were prepared and measured using One Step TUNEL Apoptosis Assay Kit (Beyotime) following the manufacturer's instructions. DNA fragmentation (staining green) was examined using a fluorescence microscope (Nikon

Eclipse-Ti, Tokyo, Japan).

2.7. Autophagy assay

GFP-LC3 HeLa cells treated with compounds or DMSO were fixed and viewed under a fluorescence microscope. Images from at least three different fields per sample were acquired, and the cells with GFP-LC3 puncta (≥ 5 dots) were calculated and analyzed using ImageJ software. In all, 20-30 cells were evaluated from each image for each sample, and three independent experiments were performed to generate the graphed values. For free GFP assay, cells treated with or without compounds were subjected to Western blot analysis using an antibody against GFP.

2.8. Acridine orange (AO) staining

Cells grown on coverslips were treated with DMSO or 10 μ M CC for 24 h, and then stained with the pH-sensitive fluorescent dye AO (5 μ g/ml in PBS) at 37°C for 10 min. After washing twice with PBS, samples were viewed under a confocal fluorescence microscope (Nikon D-Eclipse C1).

2.9. Immunofluorescence microscopy

Cells were grown on coverslips and fixed in 3% (w/v) paraformaldehyde (PFA) in PBS at room temperature (RT) for 20 min. PFA fixed cells were quenched with 10 mM glycine (pH 8.5) in PBS, and permeabilized with 0.1% Triton X-100 for 4 min at RT. Coverslips were incubated for 60 min at RT with primary antibodies diluted into PBS containing 0.5 mg/mL

BSA. After washing with PBS, the cells were incubated with fluorophore-conjugated secondary antibodies diluted in PBS for a further 30 min at RT. Counterstaining of nuclei was done with Hoechst 33342 (Sigma). Coverslips were sealed with Mowiol and dried in the dark. Cells were imaged under the confocal microscope and image analysis was performed using ImageJ software.

2.10. RNA interference

pLKO.1-puro lentiviral vectors expressing TFEB shRNA (5'-CCGGCCCACTTTGGTGCTAATAGCTCTCGAGAGCTATTAGCACCAAAGTGGGTTT TTG-3') and pLKO.1-puro lentiviral vectors expressing ATG7 shRNA (5'-CCGGCCCAGCTATTGGAACACTGTACTCGAGTACAGTGTTCCAATAGCTGGGTTT TT-3') were constructed and the knockdown level was tested by Western blot. The non-target shRNA control vector (SHC002) was obtained from Sigma. Lentiviruses were produced according to the manufacturers' manual. Cells were infected with lentiviruses and selected in 1 µg/ml puromycin for at least two weeks.

2.11. Real-time PCR (qPCR)

Total RNA was extracted from cells using a Trizol reagent (Invitrogen) according to the manufacturer's protocol. RNA was reverse-transcribed into cDNAs using Revert Aid First Strand cDNA Synthesis kit (Thermo Scientific). The qPCR was performed on an ABI Prism 7900HT Real-Time PCR System (Applied Biosystems, Carlsbad, CA, USA) using Fermentas Maxima SYBR Green/ROX qPCR reagents (Thermo Fisher Scientific). The reactions were

carried out in a 96-well plate at 95 °C for 10 min, followed by 40 cycles of 95 °C for 15 s and 60 °C for 30 s. GAPDH expression was used as an endogenous control to normalize target gene expression by the $\Delta\Delta C_t$ method. Primers used were as follows: TFEB, 5'-AACAGTGCTCCCAATAGCCC-3' and 5'-TGGGGATCAGCATTCCCAAC-3'; CatB, 5'-ACAGCCCGACCTACAAACAG-3' and 5'-AGAAGCCATTGTCACCCCAG-3'; CatD, 5'-GACATCCACTATGGCTCGGG-3' and 5'-AGCACGTTGTTGACGGAGAT-3'; GAPDH, 5'-CAAGGTCATCCATGACAACCTTTG-3' and 5'-GTCCACCACCCTGTTGCTGTAG-3'.

2.12. Statistical analysis

Statistical significance was analyzed by one-way analysis of variance (ANOVA), followed by Tukey's test using Origin85 software. In all cases, $P < 0.05$ was considered statistically significant.

3. Results

3.1. CC induces TFEB nuclear translocation

Using HeLa cells stably expressing a TFEB-GFP fusion protein, we screened and found that CC treatment potently induced TFEB-GFP nuclear translocation. The spatio-temporal kinetics of TFEB-GFP nuclear translocation was analyzed via exposing the cells to CC (1-20 μM) for 6, 12 and 24 h (data not shown). The localization of TFEB-GFP was observed under a fluorescence microscope. Significant nuclear accumulation of TFEB-GFP was observed after treatment with 10 μM CC for 12 or 24 h, compared to the control (Fig. 1A). Similar results

were also observed upon treatment with the known mTORC1 inhibitor Torin1 (200 nM, 2 h). To further confirm the nuclear translocation of endogenous TFEB in response to CC treatment, subcellular fractionation and Western blot were performed using HeLa and MDA-MB-231 cells. After the treatment with 10 μ M CC for 24 h, nuclear TFEB protein level was significantly increased in these cell lines (Fig. 1B and C). These results indicate that CC induces TFEB nuclear translocation. Moreover, tamoxifen (15 μ M), a AEBS ligand, also induced TFEB nuclear translocation after 12 h or 24 h treatment in HeLa cells (Fig. 1D). The expression of estrogen receptor- α (ER α) was examined in MCF-7, HeLa and MDA-MB-231 cells, the result showed that HeLa and MDA-MB-231 cells were ER negative (Fig. 1E). In addition, the expression of TFEB with CC treatment (10 μ M, 24 h) were detected by Western blot and qPCR, respectively. The results showed that CC increased the protein level of TFEB in HeLa and MDA-MB-231 cells (Fig. 1F), however, the mRNA level of TFEB was not affected by CC treatment (Fig. 1G).

3.2. CC inhibits cell viability

To address the effect of CC on cell viability, MTT assays were performed in HeLa and MDA-MB-231 cells. As shown in Fig. 2A and B, CC inhibited the growth of aforementioned cells in a dose- and time-dependent manner. After 48 h and 72 h treatment with CC, the IC₅₀ values were 10.93 and 8.63 μ M for HeLa cells, 10.84 and 5.90 μ M for MDA-MB-231 cells respectively. 10 μ M of CC significantly suppressed the viability of cancer cells by about 50% upon 48 h of treatment (Fig. 2A and B). To investigate whether the activation of TFEB is directly involved in CC-induced growth inhibition, we knocked down TFEB using shRNA

(shTFEB) in HeLa or MDA-MB-231 cells. As shown in Fig. 2C and E, shRNA-mediated knockdown of TFEB led to a significant decrease of TFEB protein level, which effectively rescued the CC-induced growth inhibition at 48 and 72 h, compared to the control (Fig. 2D and F). Moreover, CC treatment (10 μ M, 48 h) increased the levels of cell cycle protein p27 in HeLa and MDA-MB-231 cells (Fig. 2G and H), which indicated that cell cycle was inhibited by CC.

3.3. CC causes apoptosis

To investigate whether CC induces apoptosis, Annexin V/PI double staining assay was performed in HeLa and MDA-MB-231 cells. Both of them showed an obvious apoptosis after a 48 h treatment with CC (10 or 15 μ M), compared to the control (Fig. 3A and B). Based on Western blot analysis, both cleaved caspase-9 and cleaved caspase-3 levels were obviously increased in a dose-dependent manner after 48 h CC treatment (Fig. 3C and D). Furthermore, TUNEL staining showed that the DNA fragmentation was provoked after CC treatment (10 μ M, 48 h) in HeLa and MDA-MB-231 cells (Fig. 3E and F). These results suggest that CC induces intrinsic apoptotic cell death.

3.4. CC increases lysosomal proteins expression and induces LMP

It has been reported that TFEB regulates the expression of lysosomal proteins[31], we then evaluated the expression of CatB and CatD in HeLa and MDA-MB-231 cells treated with CC. Western blot analysis demonstrated an increase of CatB and CatD protein levels following 48 h treatment with 10 μ M CC. In contrast, shRNA-mediated knockdown of TFEB attenuated

the CC-induced expression of CatB and CatD (Fig. 4A and B). We also detected the effect of CC treatment on the transcriptional activity of CatB and CatD. The results showed that the mRNA levels of CatB and CatD were significantly increased after 24 h treatment with 10 μ M CC (Fig. 4C and D). Moreover, we investigated whether CC treatment induces LMP in HeLa and MDA-MB-231 cells. Lysosomal proteases, such as CatB and CatD, are released from lysosomes into the cytosol induced by LMP. Cytoplasmic proteins from CC-treated cells were extracted to measure the amount of CatB and CatD released from the lysosome. Western blot showed that the cytoplasmic CatB and CatD levels were increased in the presence of CC (10 μ M, 48 h), compared to the control (Fig. 4E and F). In contrast, Western blot analysis showed that depletion of TFEB markedly attenuated the CC-induced release of CatB and CatD from the lysosome (Fig. 4G and H). These results indicate that CC induces lysosomal proteins expression and causes LMP.

3.5. CC treatment induces autophagy

It has been reported that TFEB may regulate autophagy by driving expression of autophagy genes[17]. HeLa cells stably expressing a GFP-LC3 fusion protein were used to evaluate the impact of CC treatment in autophagy. The fluorescence detection showed that CC treatment (10 μ M, 24 h) significantly increased the number of GFP-LC3 puncta (Fig. 5A), suggesting that the number of autophagosomes increased in response to CC treatment. This observation was further supported by Western blot analysis showing that CC treatment resulted in a significant increase in the abundance of LC3-II in a dose- and time-dependent manner (Fig. 5B and C). However, CC treatment did not result in a significant decrease in the abundance of

p62. In addition, autophagy flux was monitored in the CC-treated HeLa cells stably expressing GFP-LC3. The GFP-LC3 fusion protein is partially degraded upon reaching the lysosome, resulting in the appearance of a free GFP fragment. Therefore, it has been suggested that the detection of free GFP fragments can be used to measure autophagic flux because GFP is more stable than the GFP-LC3 fusion protein in the acidic lysosomal compartment[32]. The free GFP fragment were increased in a dose-dependent manner following CC treatment (Fig. 5D). These results indicate that CC treatment induces autophagy.

3.6. CC-induced autophagy promotes cell death via LMP

To evaluate the role of autophagy in CC-induced cell death, we knocked down ATG7 using shRNA (shATG7) in HeLa cells. As shown in Fig. 6A, shRNA-mediated knockdown of ATG7 resulted in a significant decrease in ATG7 protein level, which effectively reduced the abundance of LC3-II in cells treated with 10 μ M CC for 48 h. Moreover, Western blot data showed that depletion of ATG7 markedly decreased the CC-induced activation of caspase-3, indicating that CC-induced autophagy contributes to the apoptosis event. Further MTT analysis revealed that ATG7 knockdown rescued the cells from CC-induced growth inhibition, compared to the control (Fig. 6B). Furthermore, we detected the role of ATG7 knockdown in CC-induced LMP, and found that depletion of ATG7 markedly attenuated the release of CatB and CatD from the lysosome after CC treatment (10 μ M, 48 h) (Fig. 6C).

3.7. CC induced-nuclear translocation of TFEB regulates lysosomal biogenesis independent of mTORC1

To detect whether the CC induced-nuclear translocation of TFEB regulates lysosomal

biogenesis, AO staining assay was performed in HeLa cells after CC treatment. The result showed that CC treatment (10 μ M, 24 h) resulted in a significant increase in the abundance of acidic organelles (Fig. 7A). Lysosomes were stained using lysosome associated membrane protein (LAMP) 2 antibody, and data revealed an increase in the number and in the size of lysosomes following CC treatment (Fig. 7B). Furthermore, we examined the effect of CC on mTORC1 activity. Whereas Torin1 (200 nM, 12 h) clearly inhibited the phosphorylation of p70 S6 kinase (S6K), a known mTORC1 substrate[33], CC (10 μ M, 24 h) did not change the phosphorylation of S6K in HeLa and MDA-MB-231 cells (Fig. 7C and D). These results indicate that CC-induced TFEB translocation and lysosomal biogenesis are independent of mTORC1.

4. Discussion

CC, a nonsteroidal triphenylethylene compound, is a first line of medicine used for the induction of ovulation[24]. CC can be used to induce follicular maturation and ovulation in polycystic ovarian syndrome[34], lead to oocyte apoptosis[28] and alleviate the condition of patients with breast cancer[35]. The present study show that CC as a TFEB activator increases lysosomal biogenesis and promotes autophagy flux in model cells. Duo to both HeLa and MDA-MB-231 are ER-negative cell lines, CC induces TFEB activation through ER independent pathways. Simultaneously, CC treatment specifically causes a leak of lysosomal protease CatB and CatD into the cytoplasm, resulting in cell death through apoptosis. Inhibition of autophagy by ATG7 knockdown significantly decreases the CC-induced LMP and cell death.

As the impairment of lysosomal degradative machinery has been mechanistically associated with neurodegenerative diseases[36], metabolic disorders[3, 7] and aging[4, 9], enhancing this innate cellular clearance machinery offers a new therapeutic strategy for treatment of these diseases. The transcription factor TFEB acts as a master regulator of cellular clearance through enhancement of the autophagy-lysosome pathway, including lysosomal biogenesis[11], expression of autophagy genes[17] and lysosomal proteostasis[31]. Consequently, TFEB agonists are of interest for potential therapeutic intervention for some metabolic disorders or ageing. In this study, we found that CC, a FDA-approved drug for the treatment of female infertility, promotes nuclear translocation of TFEB and increases lysosomal biogenesis in an mTORC1-independent manner. At the lysosome, mTORC1 directly represses the activation of TFEB by phosphorylation at serine 211 site[14, 16]. Although inhibition of mTORC1 can activate TFEB, mTORC1 is not an ideal drug target, due to its pivotal roles in regulating multiple cell growth and anabolic function. Our observation may represent a potential candidate for the pharmacological modulation of lysosomal function, though further studies are required to fully elucidate the mechanism underlying CC-mediated TFEB nuclear translocation. Interestingly, CC and other AEBS ligands stimulate the production of ROS in breast cancer cells[30], thus, a possible mechanism is that the production of ROS is involved in TFEB translocation in response to CC treatment. Consistent with this prediction, recent studies suggest that increasing ROS levels directly activate lysosomal MCOLN1 (a member of the transient receptor potential channel family) to induce lysosomal Ca^{2+} release, triggering calcineurin-dependent TFEB nuclear translocation to

enhance autophagy[37]. Alternatively, AEBS is located in the endoplasmic reticulum (ER) of cells, where it carries out the cholesterol-5,6-epoxide hydrolase activity that are involved in the late stages of cholesterol biosynthesis[38]. It has been established that ER stress leads to the activation of PERK (double-stranded RNA-activated protein kinase (PKR)-like ER kinase) and calcineurin, causing translocation of TFEB to the nucleus in a mTORC1-independent mechanism[39]. Hence, more studies are needed to clarify whether ER stress also contributes to TFEB activation induced by CC or other AEBS ligands.

In our study, CC treatment upregulates the expression of TFEB at protein level, but not at mRNA level. A possible explanation is that CC promotes TFEB nuclear translocation and changes its post-translational modification, resulting in the stability of TFEB protein in cells. Consistent with this interpretation, STUB1, a chaperone-dependent E3 ubiquitin ligase, modulates TFEB activity by preferentially targeting inactive phosphorylated TFEB for degradation by the ubiquitin-proteasome pathway[40].

Although mounting experimental evidence converges on TFEB activation as a potential therapeutic target for some metabolic disorders or neurodegenerative diseases[18, 21, 23], relatively little is known about the adverse effects of these TFEB activators. In this study, we found CC treatment causes a leak of lysosomal protease CatB and CatD into the cytoplasm. LMP is a perturbation of the lysosomal membrane function leading to the translocation of lysosomal hydrolases from the lysosomal lumen to cytosol, lysosomal proteases that have been implicated in cell death are cathepsins, such as CatB, CatD and CatL, these proteases

remain active at neutral pH and activate apoptotic effectors such as mitochondria and caspases[41]. Indeed, both caspase-9 and caspase-3 activation were observed after CC treatment, suggesting that CC induces intrinsic apoptotic cell death. Interestingly, both CatB and CatD are downstream targets of the TFEB transcription factor[13]. Thus, one possible mechanism is that CC induces TFEB activation to upregulate the expression of CatB and CatD, resulting in the highly expressed proteases leaking from the lysosomes and induces the LMP-mediated cell death. On the basis of this study, multiple cellular alterations caused by TFEB activators should be considered as a risk factor for the potential use of this compound for treatment of metabolic disorders or neurodegenerative diseases. It has been reported that antioxidants, such as desferrioxamine mesylate, N-acetylcysteine and α -tocopherol, block LMP and hence prevent all subsequent steps of the apoptotic cascade[42]. Thus, supplementation of the antioxidants along with CC could be beneficial to overcome the adverse effect caused by CC treatment. Moreover, based on our current results, the cathepsin's inhibitors may also rescue the CC-induced apoptotic effects.

TFEB not only induces the expression of genes associated with lysosomal function but also the genes necessary for autophagosome formation[17]. Indeed, our results showed that the autophagy flux is also increased after CC treatment as the levels of both LC3-II and free GFP accumulate, although CC has little effect on the level of p62 (also known as SQSTM1, a substrate protein for autophagy pathway). Since *p62* is a direct target gene downstream of TFEB[13], it is possible that active TFEB is sufficient to maintain p62 levels, thus resulting in an unmodified form of p62 within CC-treated cells. Interestingly, we found that autophagy

might be responsible for CC-induced LMP and cell death, since ATG7 knockdown retarded the release of CatB and CatD from the lysosome and the activation of caspase-3. It still remains to be determined how CC-induced autophagy modulates LMP and this elucidation will greatly clarify the mechanism of the cellular processes impacted by the TFEB agonists.

In summary, we show here that CC promotes TFEB nuclear translocation and induces apoptosis by enhancing LMP. These findings not only provide important mechanistic insights into the adverse effect of TFEB activation, but also may lead to the development of a new strategy for the potential application of TFEB agonists in disease treatment.

Acknowledgements

Funding was provided by the Scientific and Technological Research Program of Tianjin Municipal Education Commission (Grant No. 2017KJ007). We are grateful to Dr. Edward McKenzie (The University of Manchester, UK) for the critical reading of the manuscript.

Conflict of interest

The authors declare that they have no conflict of interest related to the presented work.

References

- [1] B. Levine, D.J. Klionsky, Development by self-digestion: molecular mechanisms and biological functions of autophagy, *Dev. Cell* 6(4) (2004) 463-477.
- [2] P. Jiang, N. Mizushima, Autophagy and human diseases, *Cell Res.* 24(1) (2014) 69-79.

- [3] R. Singh, S. Kaushik, Y. Wang, Y. Xiang, I. Novak, M. Komatsu, et al., Autophagy regulates lipid metabolism, *Nature* 458(7242) (2009) 1131-1135.
- [4] D.C. Rubinsztein, G. Marino, G. Kroemer, Autophagy and aging, *Cell* 146(5) (2011) 682-695.
- [5] C. Ebato, T. Uchida, M. Arakawa, M. Komatsu, T. Ueno, K. Komiya, et al., Autophagy is important in islet homeostasis and compensatory increase of beta cell mass in response to high-fat diet, *Cell Metab.* 8(4) (2008) 325-332.
- [6] W. Quan, K.Y. Hur, Y. Lim, S.H. Oh, J.C. Lee, K.H. Kim, et al., Autophagy deficiency in beta cells leads to compromised unfolded protein response and progression from obesity to diabetes in mice, *Diabetologia* 55(2) (2012) 392-403.
- [7] L. Yang, P. Li, S. Fu, E.S. Calay, G.S. Hotamisligil, Defective hepatic autophagy in obesity promotes ER stress and causes insulin resistance, *Cell Metab.* 11(6) (2010) 467-478.
- [8] W.X. Ding, M. Li, X. Chen, H.M. Ni, C.W. Lin, W. Gao, et al., Autophagy reduces acute ethanol-induced hepatotoxicity and steatosis in mice, *Gastroenterology* 139(5) (2010) 1740-1752.
- [9] M. Hansen, A. Chandra, L.L. Mitic, B. Onken, M. Driscoll, C. Kenyon, A role for autophagy in the extension of lifespan by dietary restriction in *C. elegans*, *PLoS Genet.* 4(2) (2008) e24.
- [10] J.O. Pyo, S.M. Yoo, H.H. Ahn, J. Nah, S.H. Hong, T.I. Kam, et al., Overexpression of Atg5 in mice activates autophagy and extends lifespan, *Nat. Commun.* 4 (2013) 2300.
- [11] M. Sardiello, M. Palmieri, A. di Ronza, D.L. Medina, M. Valenza, V.A. Gennarino, et al., A gene network regulating lysosomal biogenesis and function, *Science* 325(5939) (2009) 473-

477.

- [12] M. Sardiello, A. Ballabio, Lysosomal enhancement: a CLEAR answer to cellular degradative needs, *Cell cycle* 8(24) (2009) 4021-4022.
- [13] M. Palmieri, S. Impey, H. Kang, A. di Ronza, C. Pelz, M. Sardiello, et al., Characterization of the CLEAR network reveals an integrated control of cellular clearance pathways, *Hum. Mol. Genet.* 20(19) (2011) 3852-3866.
- [14] J.A. Martina, Y. Chen, M. Gucek, R. Puertollano, MTORC1 functions as a transcriptional regulator of autophagy by preventing nuclear transport of TFEB, *Autophagy* 8(6) (2012) 903-914.
- [15] A. Roczniak-Ferguson, C.S. Petit, F. Froehlich, S. Qian, J. Ky, B. Angarola, T.C. Walther, et al., The transcription factor TFEB links mTORC1 signaling to transcriptional control of lysosome homeostasis, *Sci. Signal.* 5(228) (2012) ra42.
- [16] C. Settembre, R. Zoncu, D.L. Medina, F. Vetrini, S. Erdin, S. Erdin, et al., A lysosome-to-nucleus signalling mechanism senses and regulates the lysosome via mTOR and TFEB, *EMBO J.* 31(5) (2012) 1095-1108.
- [17] C. Settembre, C. Di Malta, V.A. Polito, M. Garcia Arencibia, F. Vetrini, S. Erdin, et al., TFEB links autophagy to lysosomal biogenesis, *Science* 332(6036) (2011) 1429-1433.
- [18] C. Settembre, R. De Cegli, G. Mansueto, P.K. Saha, F. Vetrini, O. Visvikis, et al., TFEB controls cellular lipid metabolism through a starvation-induced autoregulatory loop, *Nat. Cell Biol.* 15(6) (2013) 647-658.
- [19] J.A. Martina, R. Puertollano, Rag GTPases mediate amino acid-dependent recruitment of TFEB and MITF to lysosomes, *J. Cell Biol.* 200(4) (2013) 475-491.

- [20] D.L. Medina, A. Fraldi, V. Bouche, F. Annunziata, G. Mansueto, C. Spampanato, et al., Transcriptional activation of lysosomal exocytosis promotes cellular clearance, *Dev. Cell* 21(3) (2011) 421-430.
- [21] C. Wang, H. Niederstrasser, P.M. Douglas, R. Lin, J. Jaramillo, Y. Li, et al., Small-molecule TFEB pathway agonists that ameliorate metabolic syndrome in mice and extend *C. elegans* lifespan, *Nat. Commun.* 8(1) (2017) 2270.
- [22] H. Lim, Y.M. Lim, K.H. Kim, Y.E. Jeon, K. Park, J. Kim, et al., A novel autophagy enhancer as a therapeutic agent against metabolic syndrome and diabetes, *Nat. Commun.* 9(1) (2018) 1438.
- [23] M. Palmieri, R. Pal, H.R. Nelvagal, P. Lotfi, G.R. Stinnett, M.L. Seymour, et al., mTORC1-independent TFEB activation via Akt inhibition promotes cellular clearance in neurodegenerative storage diseases, *Nat. Commun.* 8 (2017) 14338.
- [24] E. Shalev, Y. Geslevich, M. Matilsky, M. Ben-Ami, Gonadotrophin-releasing hormone agonist compared with human chorionic gonadotrophin for ovulation induction after clomiphene citrate treatment, *Hum. Reprod.* 10(10) (1995) 2541-2544.
- [25] J.H. Clark, B.M. Markaverich, The agonistic-antagonistic properties of clomiphene: a review, *Pharmacol. Ther.* 15(3) (1981) 467-519.
- [26] T. Hayon, A. Dvilansky, L. Oriev, I. Nathan, Non-steroidal antiestrogens induce apoptosis in HL60 and MOLT3 leukemic cells; involvement of reactive oxygen radicals and protein kinase C, *Anticancer Res.* 19(3A) (1999) 2089-2093.
- [27] S.N. London, D. Young, G. Caldito, J.B. Mailhes, Clomiphene citrate-induced perturbations during meiotic maturation and cytogenetic abnormalities in mouse oocytes in

vivo and in vitro, *Fertil. Steril.* 73(3) (2000) 620-626.

[28] S.K. Chaube, P.V. Prasad, S.C. Thakur, T.G. Shrivastav, Estradiol protects clomiphene citrate-induced apoptosis in ovarian follicular cells and ovulated cumulus-oocyte complexes, *Fertil. Steril.* 84 Suppl 2 (2005) 1163-1172.

[29] B. Kedjouar, P. de Medina, M. Oulad-Abdelghani, B. Payre, S. Silvente-Poirot, G. Favre, et al., Molecular characterization of the microsomal tamoxifen binding site, *J. Biol. Chem.* 279(32) (2004) 34048-34061.

[30] P. de Medina, B. Payre, N. Boubekour, J. Bertrand-Michel, F. Terce, S. Silvente-Poirot, et al., Ligands of the antiestrogen-binding site induce active cell death and autophagy in human breast cancer cells through the modulation of cholesterol metabolism, *Cell Death. Differ.* 16(10) (2009) 1372-1384.

[31] W. Song, F. Wang, M. Savini, A. Ake, A. di Ronza, M. Sardiello, et al., TFEB regulates lysosomal proteostasis, *Hum. Mol. Genet.* 22(10) (2013) 1994-2009.

[32] N. Mizushima, T. Yoshimori, B. Levine, Methods in mammalian autophagy research, *Cell* 140(3) (2010) 313-326.

[33] N. Pullen, G. Thomas, The modular phosphorylation and activation of p70s6k, *FEBS Lett.* 410(1) (1997) 78-82.

[34] R.F. Savaris, J.M. Groll, S.L. Young, F.J. DeMayo, J.W. Jeong, A.E. Hamilton, et al., Progesterone resistance in PCOS endometrium: a microarray analysis in clomiphene citrate-treated and artificial menstrual cycles, *J. Clin. Endocrinol. Metab.* 96(6) (2011) 1737-1746.

[35] E. Hecker, I. Vegh, C.M. Levy, C.A. Magin, J.C. Martinez, J. Loureiro, et al., Clinical trial of clomiphene in advanced breast cancer, *Eur. J. Cancer* 10(11) (1974) 747-749.

- [36] J. Nah, J. Yuan, Y.K. Jung, Autophagy in neurodegenerative diseases: from mechanism to therapeutic approach, *Mol. Cells* 38(5) (2015) 381-389.
- [37] X.L. Zhang, X.P. Cheng, L. Yu, J.S. Yang, R. Calvo, S. Patnaik, et al., MCOLN1 is a ROS sensor in lysosomes that regulates autophagy, *Nat. Commun.* 7 (2016).
- [38] P. de Medina, M.R. Paillasse, G. Segala, M. Poirot, S. Silvente-Poirot, Identification and pharmacological characterization of cholesterol-5,6-epoxide hydrolase as a target for tamoxifen and AEBS ligands, *Proc. Natl. Acad. Sci. U S A* 107(30) (2010) 13520-13525.
- [39] J.A. Martina, H.I. Diab, O.A. Brady, R. Puertollano, TFEB and TFE3 are novel components of the integrated stress response, *EMBO J.* 35(5) (2016) 479-495.
- [40] Y.B. Sha, L. Rao, C. Settembre, A. Ballabio, N.T. Eissa, STUB1 regulates TFEB-induced autophagy-lysosome pathway, *EMBO J.* 36(17) (2017) 2544-2552.
- [41] P. Boya, G. Kroemer, Lysosomal membrane permeabilization in cell death, *Oncogene* 27(50) (2008) 6434-6451.
- [42] Y. Zang, R.L. Beard, R.A.S. Chandraratna, J.X. Kang, Evidence of a lysosomal pathway for apoptosis induced by the synthetic retinoid CD437 in human leukemia HL-60 cells, *Cell Death. Differ.* 8(5) (2001) 477-485.

Figure legends

Fig. 1. CC promotes TFEB nuclear translocation in HeLa and MDA-MB-231 cells. (A)

Analysis of TFEB-GFP nuclear translocation. HeLa cells stably expressing TFEB-GFP were cultured in full medium with or without CC for indicated time points. The fluorescent signals of TFEB-GFP were sequentially acquired by fluorescence microscopy. Cells treated with Torin1 were used as a positive control. Hoechst staining (blue) was used to identify nuclei. Representative fluorescence images are presented. Comparable results were obtained in at least three independent experiments. Scale bar, 20 μm . (B) and (C) Effects of CC on nuclear localization of endogenous TFEB. HeLa or MDA-MB-231 cells were treated with or without CC. Western blot was used to detect TFEB protein levels in the nuclear and cytoplasmic fractions. Lower panels indicate densitometric analysis of Western blot by ImageJ software. TFEB values were normalized to nuclear marker Lamin A. (D) Effects of tamoxifen on nuclear localization of TFEB. HeLa cells stably expressing TFEB-GFP were treated with or without tamoxifen for indicated time points. The fluorescent signals of TFEB-GFP were sequentially acquired by fluorescence microscopy. (E) The expression of ER α was detected using Western blot in HeLa and MDA-MB-231 cells. MCF-7 cells were used as a positive control. ER α values were normalized to β -actin. (F) The expression of TFEB with or without CC treatment was detected using whole cell lysates by Western blot. TFEB values were normalized to β -actin. (G) Effects of CC on TFEB mRNA expression. The levels of TFEB mRNA were examined in CC-treated cells by qPCR, and GAPDH was used as loading control. Data are presented as mean \pm SD of three independent experiments (* $P < 0.05$, ** $P < 0.01$, N.S.: not significant).

Fig. 2. CC induces growth inhibition in HeLa and MDA-MB-231 cells. (A) and (B) Effects of

CC on the viability of cancer cells. Cells were incubated with increasing doses of CC for 48 h, or were treated with or without 10 μ M CC for the indicated time periods. The cell viability was determined by MTT assay. The normalized value of cell viability from the untreated cells was arbitrarily set as 1.0. The results from at least three biological replicates are presented as means \pm SD (** P<0.01). (C) Knockdown of TFEB in HeLa cells stably expressing TFEB shRNA (shTFEB) or negative control shRNA (NC) was determined by Western blot using an antibody against TFEB. β -actin was used as the loading control. TFEB values were normalized to β -actin. (D) HeLa cells stably expressing shTFEB or NC shRNA were treated with or without 10 μ M CC. Cell viability was analyzed by MTT assay. (E) Depletion of TFEB in MDA-MB-231 cells stably expressing shTFEB or NC shRNA was determined by Western blot. (F) MDA-MB-231 cell line stably expressing shTFEB or NC shRNA was used to measure cell viability changes by MTT assay after CC treatment. (G) and (H) The protein levels of p27 were examined in HeLa and MDA-MB-231 cells with CC treatment. The p27 values were normalized to β -actin. The results from at least three biological replicates are presented as means \pm SD (* P<0.05, ** P<0.01).

Fig. 3. Effects of CC on cancer cells apoptosis. (A) and (B) HeLa or MDA-MB-231 cells were treated with or without CC (10 and 15 μ M) for 48 h. The percentage of cell apoptosis was determined by Annexin-V/PI staining and flow cytometry analysis. (C) and (D) Cells were treated with the indicated concentration CC for 48 h. The corresponding changes in cleaved caspase-9 and cleaved caspase-3 protein levels were measured by Western blot analysis. The caspases protein levels were normalized to β -actin. (E) and (F) DNA

fragmentation was determined by TUNEL staining after 48 h CC treatment. Data are presented as mean \pm SD of three independent experiments (* $P < 0.05$, ** $P < 0.01$).

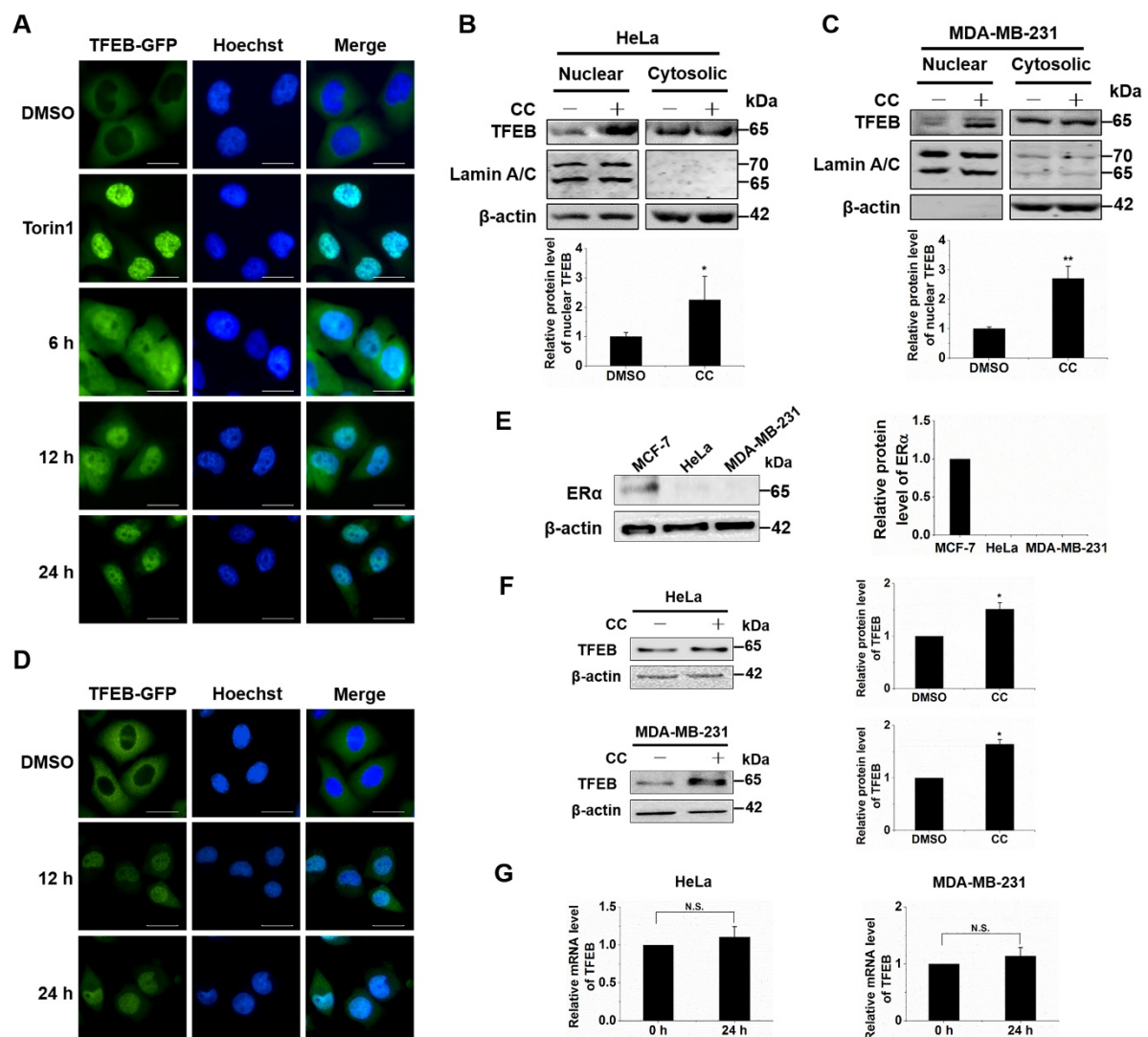
Fig. 4. Effects of CC on the expression of cathepsins and lysosomal membrane permeabilization. (A) and (B) Effects of CC treatment on CatB and CatD expression. Total proteins were extracted from HeLa or MDA-MB-231 cells stably expressing shTFEB or NC shRNA following the treatment with CC. The protein levels of CatB and CatD were detected by Western blot using an antibody against CatB or CatD. β -actin was used as a loading control. The expression of CatB and immature CatD were quantified by densitometric analysis and is represented as mean band intensity normalized to β -actin (lower panels). (C) and (D) The mRNA levels of CatB and CatD were examined in CC-treated cells by qPCR, and the values were normalized to GAPDH. (E) and (F) HeLa and MDA-MB-231 cells were treated with CC. LAMP-2, CatB, CatD and β -actin in whole cell lysate (WCL), cytosol (Cyt) and pellet (Pelt) were measured by Western blot. LAMP-2 was used as the membrane control. (G) and (H) The corresponding changes were detected in cells stably expressing shTFEB or NC shRNA following the treatment with CC. The cytosol CatB and CatD levels were quantified by densitometric analysis and normalized to β -actin. Data are presented as mean \pm SD of three independent experiments (* $P < 0.05$, ** $P < 0.01$, N.S.: not significant).

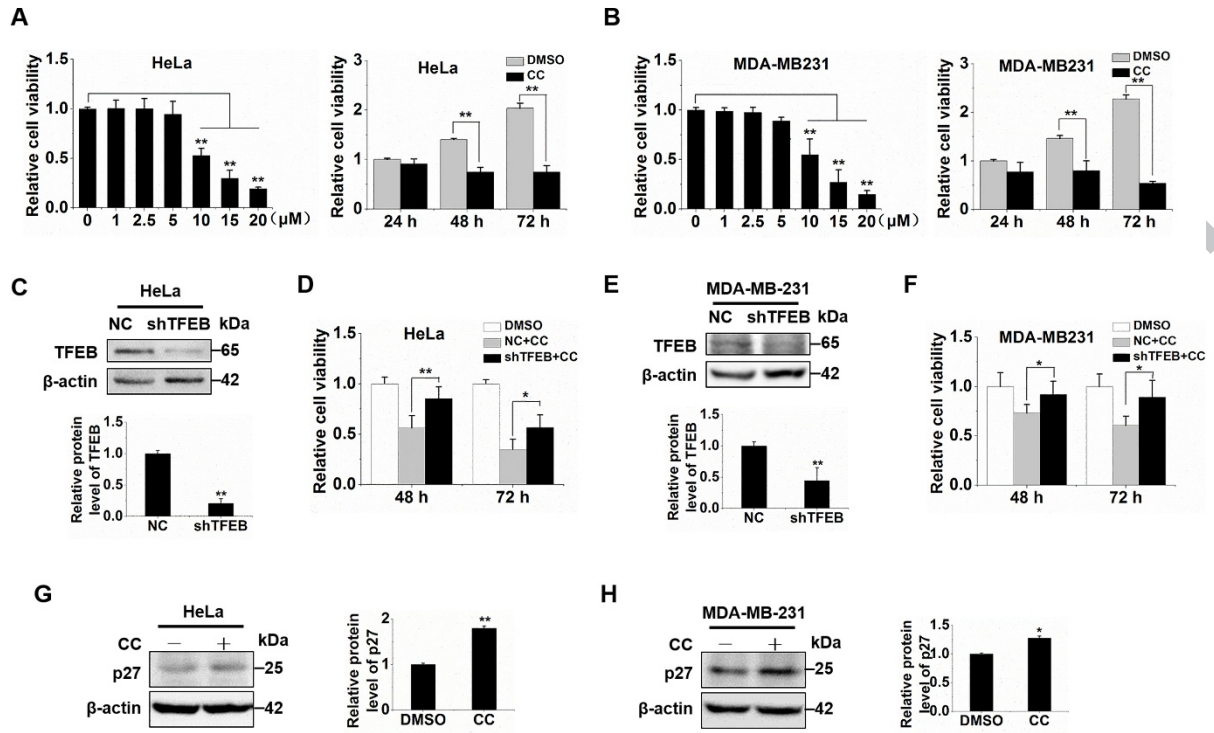
Fig. 5. CC induces autophagy. (A) HeLa cells stably expressing GFP-LC3 were treated with or without CC. The fluorescent signals of GFP-LC3 were sequentially acquired by fluorescence microscopy. Cells treated with rapamycin (Rapa, 200 nM, 12 h) were used as a

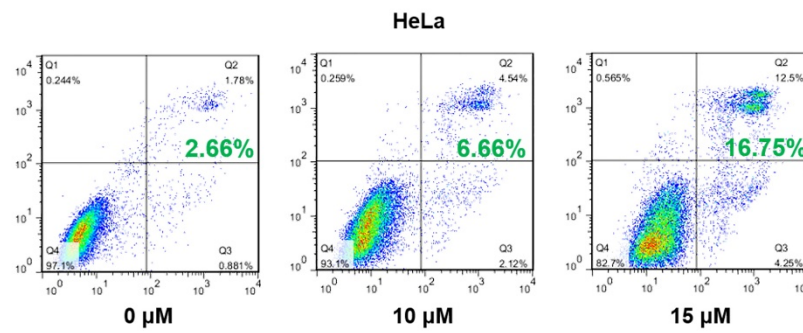
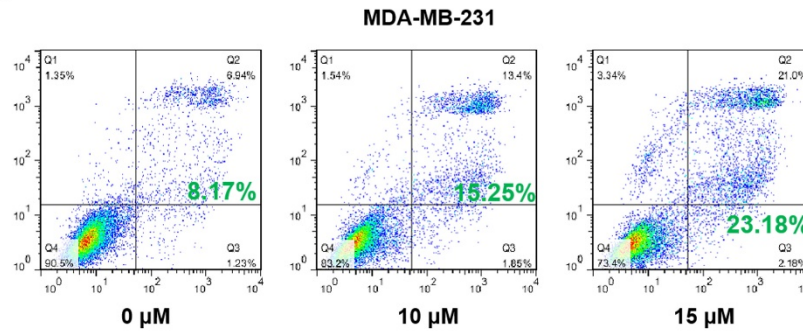
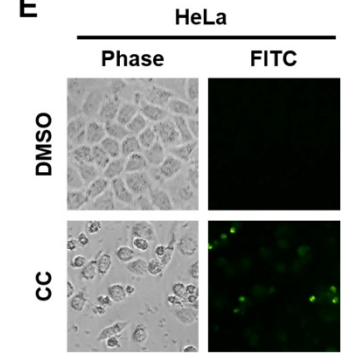
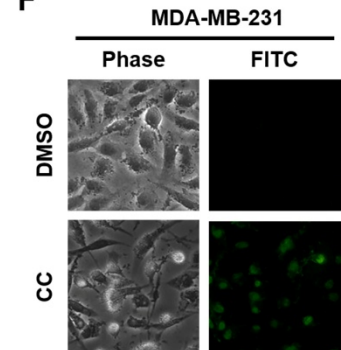
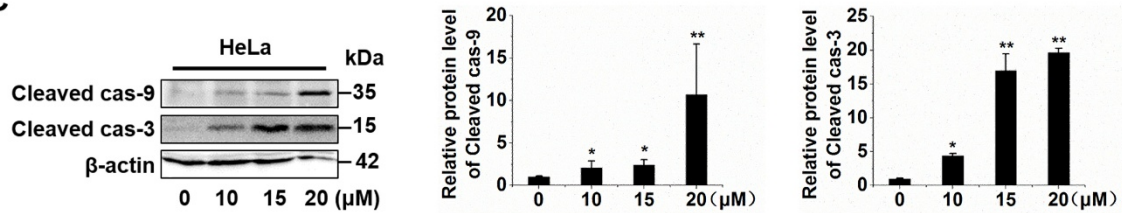
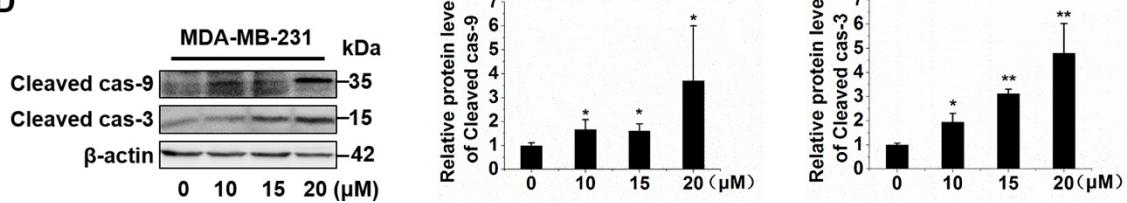
positive control. Bars, 20 μm . The percentage of cells with GFP-LC3 puncta (≥ 5 dots) was quantified. (B) and (C) Effects of CC on the expression of LC3 and p62. HeLa and MDA-MB-231 cells were treated with 10 μM CC for the indicated time points or with the indicated concentration CC for 48 h. The corresponding changes in LC3 and p62 protein levels were measured by Western blot analysis. β -actin was used as a loading control. The LC3 and p62 protein levels were normalized to β -actin. (D) Conversion of GFP-LC3 in CC-treated cells. HeLa cells stably expressing GFP-LC3 were treated with the indicated concentration of CC for 24 h. Corresponding changes in GFP-LC3 and free GFP were monitored by Western blot with an anti-GFP antibody, and GAPDH was used as loading control. Free GFP expression was quantified by densitometric analysis and is represented as mean band intensity normalized to GAPDH. Data are presented as mean \pm SD of three independent experiments (* $P < 0.05$, ** $P < 0.01$).

Fig. 6. Depletion of ATG7 rescues CC-mediated cell death. (A) HeLa cells stably expressing ATG7 shRNA (shATG7) or NC shRNA were treated with or without CC. The protein levels of ATG7, p62, LC3 and cleaved caspase-3 were measured by Western blot analysis. β -actin was used as a loading control. (B) Cell viability was analyzed by MTT assay at 48 and 72 h after 10 μM CC treatment. (C) HeLa cells stably expressing shATG7 were treated with or without CC. The levels of cytosol CatB and CatD were measured by Western blot. All protein values were normalized to β -actin. Data are presented as mean \pm SD of three independent experiments (* $P < 0.05$, ** $P < 0.01$, N.S.: not significant).

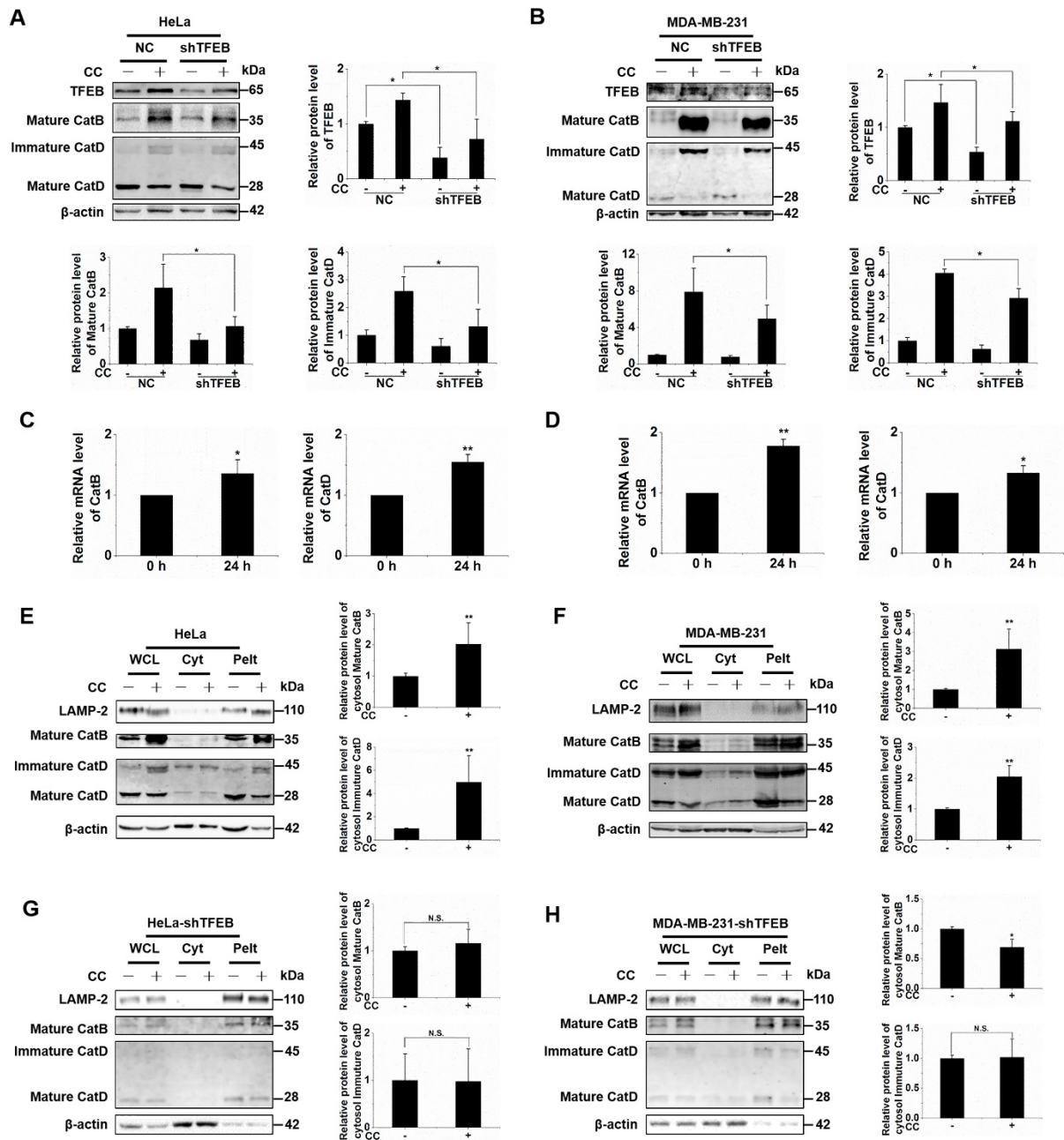
Fig. 7. Effects of CC on the lysosomal biogenesis. (A) HeLa cells were treated with or without CC. The distribution of acidic organelles was examined by AO staining and visualized using fluorescence microscopy. Torin1 were used as a positive control. (B) Cells were fixed, permeabilized and analyzed using antibody against LAMP-2 to recognize lysosomes. Scale bar, 20 μ m. (C) and (D) Western blot was used to detect the levels of phospho-S6K (p-S6K) in HeLa or MDA-MB-231 cells treated with or without CC. p-S6K values were normalized to β -actin. Data are presented as mean \pm SD of three independent experiments (* $P < 0.05$, ** $P < 0.01$, N.S.: not significant).



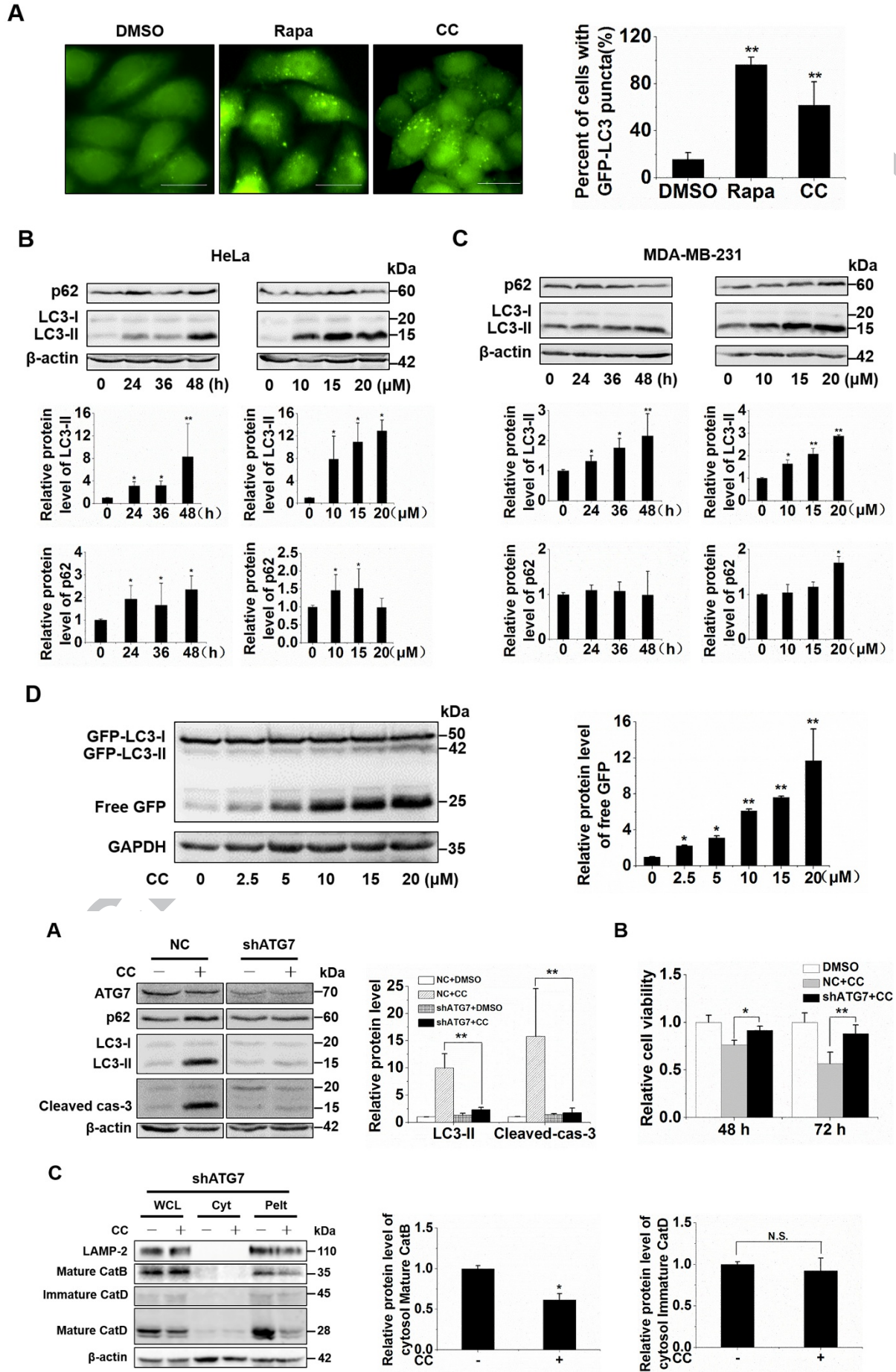


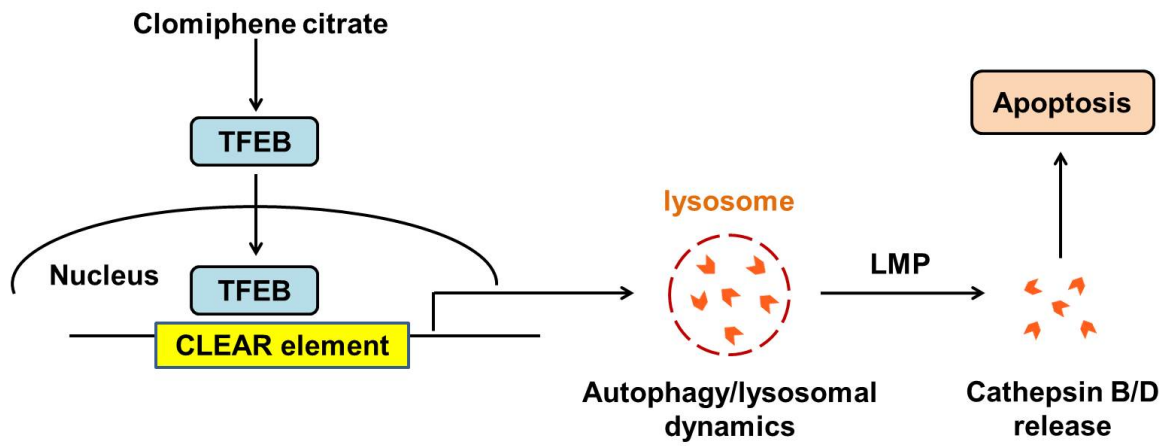
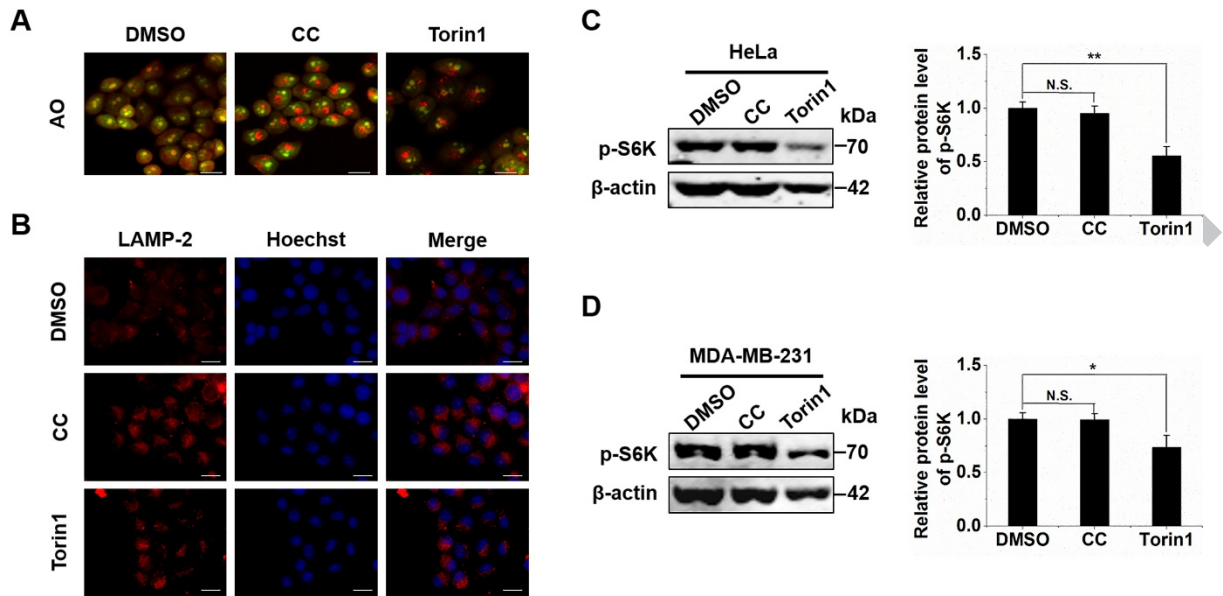
A**B****E****F****C****D**

AC



AC





ACCEPTED